

Effect of annealing temperature on the structural and optical properties of amorphous $\text{Sb}_2\text{Te}_2\text{Se}$ thin films

E. A. El-Sayad*¹ and G. B. Sakr²

¹ Physics Department, National Research Center, Dokki, Cairo, Egypt

² Physics Department, Faculty of Education, Ain Shams Univ., Cairo, Egypt

Received 31 August 2004, accepted 15 September 2004

Published online 1 November 2005

Key words semiconductors, x-ray powder diffraction, composition and phase identification, amorphous films, phase transition, optical properties.

PACS 61.10.Nz, 61.50.Nw, 61.66.Fn, 68.55.Nq, 78.66.Li

Thin films of $\text{Sb}_2\text{Te}_2\text{Se}$ were prepared by conventional thermal evaporation of the presynthesized material on Corning glass substrates. The chemical composition of the samples was determined by means of energy-dispersive X-ray spectrometry. X-ray diffraction studies on the as-deposited and annealed films revealed an amorphous-to-crystalline phase transition. The as-deposited and annealed films at $T_a = 323$ and 373 K are amorphous, while those annealed at $T_a = 423$ and 473 K are crystalline with a single-phase of a rhombohedral crystalline structure as that of the source material. The unit-cell lattice parameters were determined and compared with the reported data. The optical constants (n , k) of the investigated films were determined from the transmittance and reflectance data at normal incidence in the spectral range 400–2500 nm. The analysis of the absorption spectra revealed non-direct energy gaps, characterizing the amorphous films, while the crystalline films exhibited direct energy gaps.

© 2005 WILEY-VCH Verlag GmbH & Co. KGaA, Weinheim

1 Introduction

Metal chalcogenide semiconductors of the chemical formula $\text{V}_2\text{-VI}_3$ have shown many potential applications in optoelectronic, thermoelectric and photoelectric devices and solar selective coatings. They exhibit also several phenomena applicable for devices such as electrical switches and memories [1, 2].

So, the $\text{V}_2\text{-VI}_3$ compounds in thin films form are of great and continuous interest for investigators. Amongst these compounds, Sb_2Se_3 and Sb_2Te_3 , which crystallize in the orthorhombic and rhombohedral type structure with energy gap 1.2 and 0.3 eV; respectively [3]. Such compounds have been widely studied [4–7] where they exhibited potentially useful applications in optical storage [8, 9] and thermoelectric cooling devices [10, 11].

Some physical studies on single crystal samples of $\text{Sb}_2\text{Te}_{3-x}\text{Se}_x$ solid solutions have been reported [12–17], however the information about their thin films is rather scarce. The electrical and optical properties of $(\text{Sb}_2\text{Se}_3)_2(\text{Sb}_2\text{Te}_3)_1$ thin films have been recently reported [18]. The present work reports the effect of thermal annealing on the structural and optical properties of amorphous $\text{Sb}_2\text{Te}_2\text{Se}$ thin films.

2 Experimental techniques

Polycrystalline ingot of $\text{Sb}_2\text{Te}_2\text{Se}$ was synthesized by the direct fusion of a mixture of its constituent elements (99.999% pure antimony, tellurium, and selenium) in stoichiometric ratio, in vacuum-sealed silica tubes, using the uniform zone of an electric furnace. The temperature of the furnace was first slowly increased at a rate of 30 K h^{-1} up to 748 K, at which the mixture was left for 12 hours. Then, the temperature was increased at a rate of 40 K h^{-1} up to 1173 K, at which the entire contents were completely melted, and the melt was subjected to occasional shaking to ensure homogeneity. The temperature was then decreased at a rate of 60 K h^{-1} down to 1023 K, and the melt was then kept at this temperature for 12 hours in order to assure compound formation and homogeneity. Finally, the temperature was decreased at a rate of 30 K h^{-1} to 618 K, below which the melt was left to cool down to room temperature (300 K).

* Corresponding author: e-mail: el_sayad1@yahoo.co.uk

Thin films were deposited by conventional thermal evaporation of the synthesized material onto Corning glass substrates at room temperature (290 K), in $\sim 5 \times 10^{-4}$ Pa vacuum, using a high vacuum coating unit (Edwards 306 A). The deposition rate was kept constant during the evaporation process at nearly 3 nm/s. The film thickness, t , was monitored by a quartz crystal thickness monitor (Edwards, FTM4) and it was also measured interferometrically [19]. The as-deposited films were annealed at 323, 373, 423, and 473 K for 1 h under a vacuum of $\sim 1.5 \times 10^{-1}$ Pa.

The elemental composition of the bulk material as well as the as-deposited films was determined using an energy-dispersive X-ray spectrometer (EDXS) unit, interfaced to a scanning electron microscope (SEM; Philips XL) operating at an accelerating voltage of 30 kV. The relative error of determining the indicated elements does not exceed 5%. X-ray diffraction (XRD) of the synthesized material and the investigated films were carried out at 290 K using an automatic X-ray diffractometer (Philips Type X'Pert) with Ni-filtered, $\text{CuK}\alpha$ ($\lambda_1 = 1.54056 \text{ \AA}$) radiation operated at 30 mA and 40 kV.

The optical transmittance, T , and reflectance, R , of the films, were measured at room temperature (290 K) with unpolarized light at normal incidence in the wavelength range of 400–2500 nm using a double beam spectrophotometer (JASCO Corp., Model V-570).

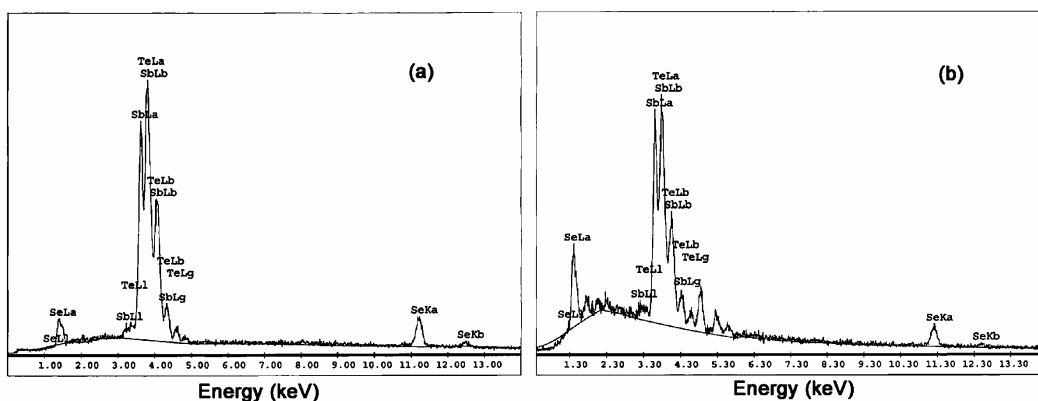


Fig. 1 EDXS spectra of $\text{Sb}_2\text{Te}_2\text{Se}$: (a) in powdered form, (b) as-deposited films on the polished surface of graphite stub.

Table 1 Elemental compositions of $\text{Sb}_2\text{Te}_2\text{Se}$ compound in powder and thin-film form compared to the calculated values.

Element	Elemental composition at. %		
	Bulk (obs.)	Thin films (obs.)	Calculated
Sb	39.72	40.57	40
Te	39.58	37.29	40
Se	20.70	22.14	20

3 Results and discussions

3.1 Structural properties

The elemental analysis of the bulk material of $\text{Sb}_2\text{Te}_2\text{Se}$ has led to the chemical formula $\text{Sb}_{1.986}\text{Te}_{1.979}\text{Se}_{1.035}$ revealing a very nearly stoichiometric composition. Also, the as-deposited films revealed the formula $\text{Sb}_{2.028}\text{Te}_{1.865}\text{Se}_{1.107}$ indicating a deficiency in Te (~ 2.71 at. %) with a slight excess of Sb (~ 0.57 at. %) and Se (~ 2.14 at. %) (see table 1 & fig. 1). The deviation from stoichiometry in thin films is comparable with the experimental error; consequently, the composition could be considered as nearly stoichiometric.

The X-ray powder diffractogram of the synthesized material in a fine powder form (Fig. 2) shows a polycrystalline structure, in quite well agreement with the standard XRD data for $\text{Sb}_2\text{Te}_2\text{Se}$ [(JCPDS card No. 71-0394), with $a = 4.188(1)$ and $c = 29.937(6) \text{ \AA}$] with rhombohedral system [20] (see table 2). The good matching between the observed reflecting planes and that of the standard data revealed that the powder diffraction trace showed no extra peaks corresponding to any precipitation of elements or binary alloys along the whole measured 2θ ranges, indicating complete miscibility of the constituent elements.

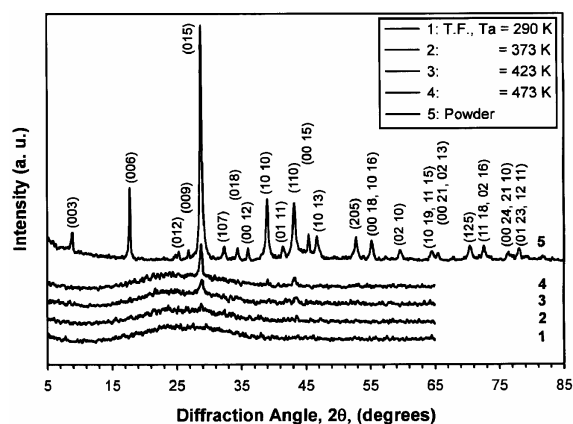


Fig. 2 XRD traces of $\text{Sb}_2\text{Te}_2\text{Se}$ in powder: 5, and thin films form: 1, as-deposited; 2, $T_a = 373$ K; 3, $T_a = 423$ K; 4, $T_a = 473$ K.

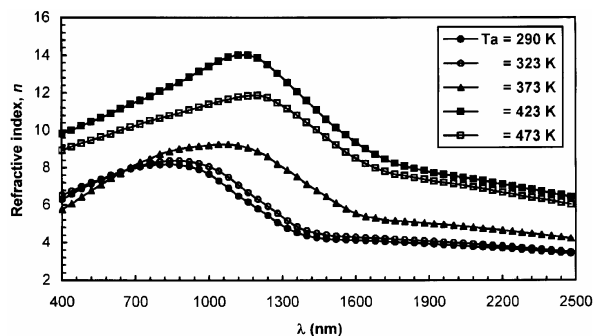


Fig. 3 Spectral behaviour of refractive index, n , for as-deposited and annealed films of $\text{Sb}_2\text{Te}_2\text{Se}$.

Table 2 X-ray analysis of $\text{Sb}_2\text{Te}_2\text{Se}$ in powder and thin-films form compared to the reported values in JCPDS card No. (71-0394) [20].

Experimental data		Thin film		Standard (JCPDS) Card no. (71-0394)		
Powder						
$d(\text{Å})$	I/I_0 %	$d(\text{Å})$	I/I_0 %	$d(\text{Å})$	I/I_0 %	hkl
9.97218	7.36	-----	-----	9.9790	1.7	003
4.98562	29.72	-----	-----	4.9895	8.9	006
-----	-----	-----	-----	3.6000	1.9	101
3.55089	1.51	-----	-----	3.5249	4.1	012
3.32087	4.1	-----	-----	3.3263	0.7	009
3.09975	100	3.09257	100	3.1021	100	015
2.76562	4.94	-----	-----	2.7661	6.2	107
2.60356	4.78	-----	-----	2.6043	5.3	018
2.49104	5.36	-----	-----	2.4947	1.8	00 12
2.30538	25.56	2.30133	9.59	2.3087	27.8	10 10
2.17850	5.44	-----	-----	2.1768	4.9	01 11
2.09208	23.07	2.08514	14.74	2.0940	31.0	110
1.99444	9.78	-----	-----	1.9958	2.9	00 15
1.94417	9.20	-----	-----	1.9440	6.9	10 13
-----	-----	-----	-----	1.9308	3.1	116
1.73406	9.11	-----	-----	1.7356	13.6	205
-----	-----	-----	-----	1.6695	1.3	027
1.66185	7.64	-----	-----	1.6631	4.9	00 18, 10 16
-----	-----	-----	-----	1.6319	0.9	208
-----	-----	-----	-----	1.6038	2.3	11 12
-----	-----	-----	-----	1.5841	0.8	01 17
1.55154	3.46	-----	-----	1.5510	6.1	02 10
-----	-----	-----	-----	1.5091	1.2	20 11
1.44501	3.63	-----	-----	1.4447	4.8	10 19, 11 15
1.42396	2.85	-----	-----	1.4247	2.1	00 21, 02 13
-----	-----	-----	-----	1.3836	0.7	01 20, 20 14
1.33557	5.46	-----	-----	1.3362	9.0	125
-----	-----	-----	-----	1.3054	1.1	217
1.30178	5.40	-----	-----	1.3023	6.5	11 18, 02 16
1.24585	2.84	-----	-----	1.2463	4.6	00 24, 21 10
1.22381	4.50	-----	-----	1.2251	3.3	01 23, 12 11
1.20727	0.85	-----	-----	1.2089	3.2	300
1.17807	0.82	-----	-----	1.1779	2.3	11 21, 21 13

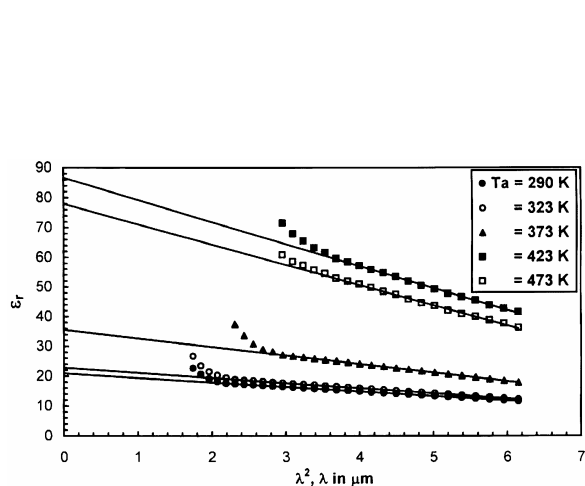


Fig. 4 Plot of ϵ_r against λ^2 for the indicated samples.

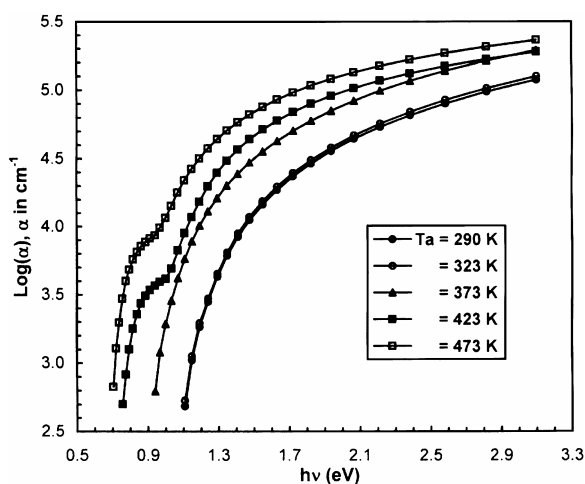


Fig. 5 Optical absorption spectra for as-deposited and annealed films of Sb₂Te₂Se.

The observed reflecting planes were indexed and the lattice parameters were determined using the CRYSFIRE 2002 computer program [21]. The determined lattice parameters $a = 4.1858$ and $c = 29.9143$ Å, are in good agreement with the reported values [20]. The analysis has, thus, indicated that the ingot material is a single-phase polycrystalline material corresponding to the rhombohedral type structure with space group $R\bar{3}m$ ($Z=3$).

XRD studies, carried out on the as-deposited (290 K) and annealed films at annealing temperatures $T_a = 323, 373, 423,$ and 473 K for 1 h, showed that the as-deposited and the annealed films at $T_a = 373$ K are amorphous. On the other hand, the films annealed at $T_a = 423$ and 473 K revealed a polycrystalline structure (Fig. 2). Such results indicate that thermal annealing induced an amorphous-to-crystalline transition. The analysis of X-ray data revealed that the films annealed at $T_a = 473$ K have a predominant (015) plane parallel to the substrate. Also, minor peaks of other reflecting planes (1,0,10) and (110) were observed. The unit cell lattice parameters for films annealed at 473 K were determined from the obtained data of the reflecting planes (015), (1,0,10), and (110) using the following relation, based on the hexagonal system;

$$1/d^2 = 4(h^2 + hk + k^2)/[3a^2 + (l^2/c^2)] \quad (1)$$

The average values of the determined lattice parameters, $a = 4.172$ Å and $c = 29.878$ Å, were found to be in suitable agreement with the reported values [20] confirming the domination of Sb₂Te₂Se single phase. The X-ray data for powder and crystalline films of Sb₂Te₂Se are given in table 2.

3.2 Optical properties

The optical properties of the Sb₂Te₂Se films were investigated for the as-deposited (290 K) and annealed films at 323, 373, 423, and 473 K for 1 h. The optical constants (n & k) were determined from both the measured values of T and R (after correcting for the absorptance and reflectance of the substrate) and the determined value of film thickness, t , using a simple computer program.

The optical absorption coefficient, α , could be calculated from the values of T and R [22, 23] using the following relation;

$$T = (1 - R)^2 \exp(-\alpha t) / [1 - R^2 \exp(-2\alpha t)] \quad (2)$$

The refractive index, n , could be determined from the values of R and the determined values of extinction coefficient, k ($= \alpha \lambda / 4\pi$), using the relation [22, 23];

$$R = [(n^2 - 1)^2 + k^2] / [(n^2 + 1)^2 + k^2] \quad (3)$$

Taking into account the experimental error in measuring the film thickness to be $\pm 2\%$ and in T and R to be 0.5% , the error of the adopted technique in the calculated values of n and k was estimated to be 1.0% and 0.5% ,

respectively. The optical constants n and k were found to be independent of the film thickness in the investigated range.

The dispersion of the refractive index, n , of the amorphous-to-crystalline films (Fig. 3) revealed that the refractive index increases on increasing the annealing temperature for films annealed at $T_a \leq 423$ K at certain λ . However, at $T_a = 473$ K, it was observed that the films exhibit a slightly lower value of n than those annealed at 423 K, indicating that the films annealed at 473 K are completely crystallized. It could also be observed that the refractive index, n , shows anomalous dispersion in the low wavelength range ($400 \leq \lambda \leq 1200$ nm). While for long wavelengths ($\lambda > 1200$ nm) n decreases monotonically, which may be attributed to the effect of the free carrier concentration, since a plot of $\epsilon_r = n^2 - k^2$, versus λ^2 (Fig. 4) exhibit a straight line in accordance with the relation [24],

$$\epsilon_r = \epsilon_\infty - (e^2 / 4\pi^2 c^2 \epsilon_0)(N / m^*)\lambda^2 \tag{4}$$

where $\epsilon_\infty = n_\infty^2$, e is the electronic charge, c is the speed of light, ϵ_0 is the permittivity of free space, N is the charge carrier concentration, and m^* is the effective mass. The high frequency dielectric constants, ϵ_∞ , and the ratio N/m^* , could be deduced from the intercept and the slope of the straight line (Table 3).

Table 3 The optical parameters of as-deposited and annealed Sb₂Te₂Se films.

T_a (K)	ϵ_∞	N/m^* (10^{21} cm ⁻³)	E_g (eV)	E_{g2} (eV)
290	20.899	1.681	1.039	-----
323	22.840	1.915	1.040	-----
373	35.612	3.209	0.878	-----
423	86.723	8.270	0.794	1.031
473	78.045	7.617	0.753	0.954

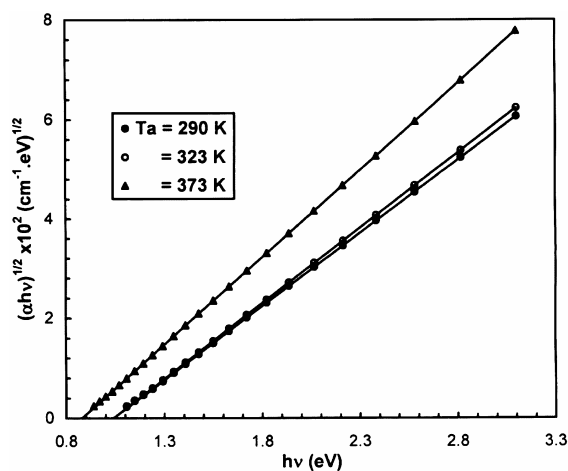


Fig. 6 Plot of $(\alpha hv)^{1/2}$ against $h\nu$ for Sb₂Te₂Se amorphous films.

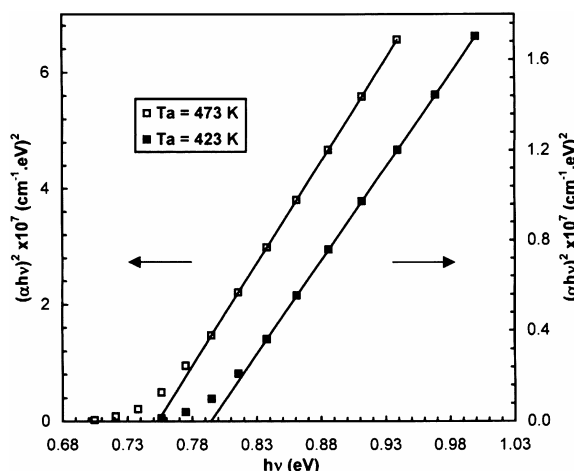


Fig. 7 Plot of $(\alpha hv)^2$ against $h\nu$ for Sb₂Te₂Se crystalline films.

The spectral behaviour of the absorption coefficient (Fig. 5) represents typical curves showing the dependence of α on photon energy, $h\nu$, and annealing temperature, T_a . The analysis of the absorption coefficients (Fig. 6) of the amorphous films was found to follow the relation;

$$\alpha(h\nu) = (A/h\nu)(h\nu - E_g)^p \tag{5}$$

with $p=2$, which characterizes a non-direct optical transition for the amorphous films according to Tauc [25]. A plot of $(\alpha hv)^{1/2}$ versus $h\nu$ yields a straight line for the as-deposited samples and films annealed at 323, and 373 K (Fig. 6) with $E_g=1.039, 1.04,$ and 0.878 eV; respectively.

The analysis of the absorption coefficient of the crystalline films (Fig. 7) annealed at $T_a=423$ and 473 K shows that the rise of α in the photon energy range $h\nu \leq 1.03$ and 0.97 eV follows the relation (5) with $p=1/2$

[26, 27]; with an energy gap $E_{g1} = 0.794$ and 0.753 eV; respectively. This transition corresponds to an allowed direct transition from the top of the valence band to the conduction band minimum at the center of the Brillouin zone. However, on calculating α_1 using A_1 and E_{g1} determined from figure 7 for energies above 1.03 and 0.97 eV we find that α_1 is considerably smaller than the absorption coefficient, α , measured experimentally, indicating the existence of additional absorption, $\alpha_2 (= \alpha - \alpha_1)$. The analysis of the additional absorption coefficient, showed that the dependence of α_2 on $h\nu$ could be described by the relation (5) with $p= 3/2$ [26, 27]; with a gap energy $E_{g2} = 1.031$ and 0.954 eV for films annealed at $T_a= 423$ and 473 K; respectively (Fig. 8). This transition corresponds to a forbidden direct transition from the crystal-field-split valence band to the conduction band minimum [28].

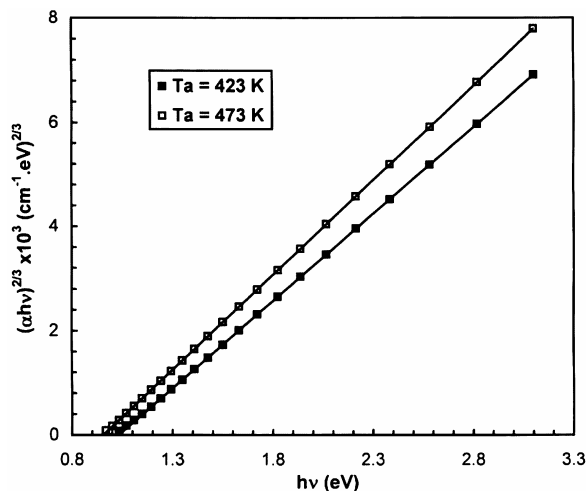


Fig. 8 Plot of $(\alpha_2 h\nu)^{2/3}$ against $h\nu$ for Sb₂Te₂Se crystalline films.

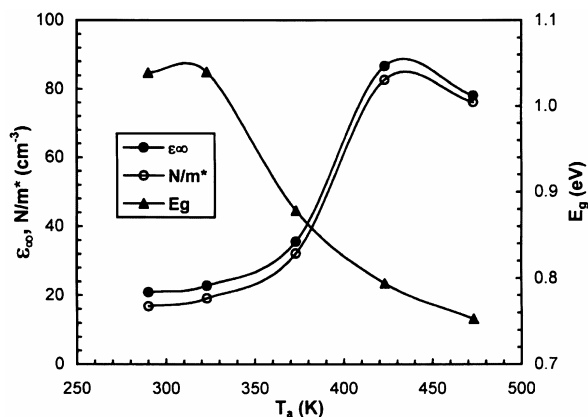


Fig. 9 Dependence of the optical parameters (ϵ_∞ , N/m^* , & E_g) of Sb₂Te₂Se films on the annealing temperature.

The annealing temperature dependence of the optical parameters (ϵ_∞ , N/m^* & E_g) of Sb₂Te₂Se films is shown in figure 9 and their determined values are given in table 3. The dependence of the fundamental optical transition energy, E_g , on the annealing temperature (Fig. 9) revealed that such energy decreases on increasing the annealing temperature for all the films exhibiting an amorphous-to-crystalline transition.

4 Conclusions

Nearly stoichiometric Sb₂Te₂Se amorphous films were deposited onto Corning glass substrates at room temperature by conventional thermal evaporation. Crystal structural analysis revealed that the as-deposited and annealed films at $T_a = 323$ and 373 K are amorphous. But an amorphous-to-crystalline phase transition with a single-phase of a rhombohedral type structure as that of the synthesized material was obtained for the annealed films in vacuum at $T_a \geq 423$ K. The optical constants (n & k) were determined from the analysis of transmittance and reflectance data. The analysis of the optical absorption spectra revealed a non-direct optical transition for the amorphous films, while direct allowed and direct forbidden transitions for the crystalline films. The annealing temperature dependence of the fundamental optical transition energy revealed that such energy decreases on increasing the annealing temperature for the investigated samples.

References

- [1] S. R. Ovshinsky, Phys. Rev. Lett. **2**, 1450 (1968).
- [2] H. Fritzsche and S. R. Ovshinsky, J. Non-Cryst. Solids. **2**, 148 (1970).
- [3] C. Wood, Rep. Prog. Phys. **51**, 459 (1988).
- [4] K. Starbova, V. Mankov, and N. Starbov, ibid. **47**, 1487 (1996).
- [5] A. P. Torane, K. Y. Rajpure, and C. H. Bhosale, Mater. Chem. Phys. **61**, 219 (1999).
- [6] A. M. Fernández and M. G. Merino, Thin Solid Films **366**, 202 (2000).
- [7] A. M. Farid, Ph.D. Thesis (1994) Cairo University.

- [8] S. Jayakumar, C. Balasubramanian, Sa. K. Narayandass, D. Mangalaraj, and C. P. Girija Vallabhan, *Thin Solid Films* **266**, 62 (1995).
- [9] P. Arun and A. G. Vedeshwar, *ibid.* **355**, 270 (1998).
- [10] B. Roy, B. R. Chakraborty, R. Bhattacharya, and A. K. Dutta, *Solid State Commun.* **25**, 617 (1978).
- [11] B. Roy, B. R. Chakraborty, R. Bhattacharya, and A. K. Dutta, *J. Phys. Chem. Solids* **41**, 913 (1980).
- [12] A. V. Ioffe and A. F. Ioffe, *Fiz. Tverd. Tela* **2**, 781 (1960).
- [13] H. A. Ullner, *Ann. Physik (Leipzig)* **21**, 44 (1968).
- [14] W. Procarione and C. Wood, *Phys. Stat. Sol.* **42**, 871 (1970).
- [15] K. Yokota and S. Katayama, *Oyo Butsuri* **41**, 706 (1972).
- [16] N. Kh. Abrikosov, V. F. Bankina, L. A. Kolomoets, and L. L. Arutyunova, *Izv. Akad. Nauk SSSR, Neorg. Mater.* **15**, **400** (1979).
- [17] P. Lostak, R. Novotny, L. Benes, and S. Civas, *J. Cryst. Growth* **94**, 656 (1989).
- [18] A. M. Farid, E. Abd El-Wahabb, and M. Fadel, *J. Mater. Sci.: Mater. Electron.* **13**, 609 (2002).
- [19] S. Tolansky, in "Multiple – Beam Interference Microscopy of Metals", (Academic Press, London, 1970) p. 55.
- [20] JCPDS-International Centre for Diffraction Data, Card number (71-0394), 1998.
- [21] R. Shirley, Crysfire 2002 program for automatic powder indexing: CCP14 website, Daresbury (<http://www.ccp14.ac.uk>).
- [22] J. I. Pankove, in "Optical Processes in Semiconductors", (Dover Publ. Inc, New York, 1971) p. 103.
- [23] T. S. Moss, G. J. Burrell, and B. Ellis, in "Semiconductor Optoelectronics", (Butterworths London, 1973) p. 10, 19.
- [24] W. G. Spitzer and N. Y. Fan, *Phys. Rev.* **106**, 882 (1957).
- [25] J. Tauc, in: "Amorphous and Liquid Semiconductors", (Plenum, New York, 1974) Ch. 4.
- [26] J. I. Pankove, "Optical Processes in Semiconductors", (Prentice-Hall, New York, 1971).
- [27] F. Bassani and G. P. Parravicini, "Electronic States and Optical Transitions in Solids", (Pergamon Press, Oxford, 1975).
- [28] L. Artus, Y. Bertrand, and C. Ance, *J. Phys. C* **19**, 5937 (1986).